Progress In Electromagnetics Research Letters, Vol. 76, 33–38, 2018

Equivalent Circuit Microwave Modeling of Graphene-Loaded Thick Films Using S-Parameters

Ololade Sanusi[1], Patrizia Savi[2, *], Simone Quaranta[3], Ahmad Bayat[2], and Langis Roy[1]

Abstract—Graphene, a one-atom thick layer of carbon atoms arranged to form a honeycomb lattice exhibits intriguing mechanical, thermal and electrical properties, which make it attractive for bio- and chemical sensors as well as flexible electronics applications. In this paper, graphene films with different amounts of graphene loading (weight fraction 12.5% and 25%) deposited by screen printing technique are characterized in the microwave frequency range. By fitting the measured scattering parameters of graphene-loaded microstrip lines with Advanced Design System (ADS) circuit simulations, a simple equivalent lumped circuit model of the film is obtained. The proposed equivalent lumped circuit model presented in this paper proves suitable as an initial step towards the full-wave electromagnetic modeling and analysis of graphene loaded microwave structures intended for sensing and tuning applications.

1. INTRODUCTION

Graphene is a 2D structure with sp^2 chemical bonding of carbon atoms arranged in a hexagonal (honeycomb) lattice [1, 2]. Electrical and mechanical properties of graphene have been widely investigated (see for example [3]).

Graphene flakes can be deposited on different substrates as thin or thick films through the preparation of inks with a proper combination of solvents and binders [4]. Graphene-based nanomaterials have gained interest due to their various applications in the terahertz region [5], in the optical range [6], for sensors development [7–9] and in the RF and microwave frequency range [10]. More recently, both graphene and carbon nanotubes have been increasingly used to develop millimeter wave components [11–13] and flexible electronics [14].

For these applications, it would be very useful to know the film impedance in the microwave range. For example, mono-atomic thick graphene can be accurately modeled as an infinitely thin surface of complex conductivity [15]. And by applying electric bias, graphene has been used for the design of reconfigurable antennas [16]. However, there has been little research done on the characterization of graphene films at radio frequencies. Only a few works can be found on the characterization of graphene-polymer composite films [17–19]. This makes it difficult to realize adequate electromagnetic models of graphene films at these frequencies.

In [20], a circuit model of graphene thick film is introduced, but the model is based only on the fitting of the amplitude of the measured scattering response. In this letter, a detailed circuit characterization of graphene films based on measurement-based modeling in 1–5 GHz band is addressed. Based on the measured scattering parameters (amplitude and phase) of a microstrip line loaded with graphene film of various compositions, a lumped element equivalent circuit is derived to describe the film impedance at microwave frequencies.

Received 9 April 2018, Accepted 10 May 2018, Scheduled 21 May 2018

* Corresponding author: Patrizia Savi (patrizia.savi@polito.it).
[1] Department of Electrical, Computer and Software Engineering, University of Ontario Institute of Technology, Oshawa, ON, Canada.
[2] Department of Electronic and Telecommunications, Politecnico di Torino, Torino, Italy. [3] Department of Electronic, information and Telecommunication Engineering, University "La Sapienza", Rome, Italy.

2. FILM PREPARATION

Screen-printing is used to deposit graphene as a thick film (each layer is about 10 μm thick) across the gap between two electrodes. The ink for screen printing is prepared according to the procedure described in [21] for 12.5% and 25% graphene by adding proper quantity of ethyl cellulose (EC) binder (Sigma Aldrich, viscosity 10 cP, 5% toluene/ethanol, 48% ethoxyl) and terpineol (Sigma Aldrich, boiling point 220°C). The chemistry of ink formulation for screen printing accounts for a homogeneous dispersion of graphene sheets into the binder matrix to ensure that the electrical and mechanical properties of graphene are translated uniformly along the film. Homogeneous dispersion also guarantees repeatability of the films. Electrical connectivity throughout the film is verified by sheet resistance measurements (see Table 1). A $3 \times 3\,\text{mm}^2$ film is printed on an FR-4 substrate through a 230 mesh/inch polyester screen. Films with thicknesses of about 30 μm are made by depositing three layers, with intermittent drying at 125°C for 5 minutes following the deposition of successive printed layers. Final curing is performed in a muffle at 160°C for 150 minutes in air.

Table 1. Measured dc sheet resistance for 12.5% and 25% weight fraction graphene film.

Sample	One-layer (Ω/sq)	Two-layer (Ω/sq)
Ethyl cellulose	$> 2 \times 10^8$	$> 2 \times 10^8$
12.5 wt.%	2×10^7	2×10^6
25 wt.%	650	440

3. EQUIVALENT MICROWAVE CIRCUIT

In order to understand the RF behavior of the deposited graphene films, a 3 mm wide microstrip line with a 2.6 mm gap spacing is photo-etched on a 1.57 mm thick FR-4 substrate (nominal dielectric constant of 4.3 and loss tangent of 0.03 at 2 GHz). The 3 mm strip width corresponds to 50 Ω characteristic impedance. Thick films ($30\,\mu\text{m} \times 3\,mm \times 3\,\text{mm}$) of ethyl cellulose binder alone, 12.5 wt.% graphene and 25 wt.% graphene, are then printed on the gap (see Fig. 1(a)) using the deposition technique described in Section 2.

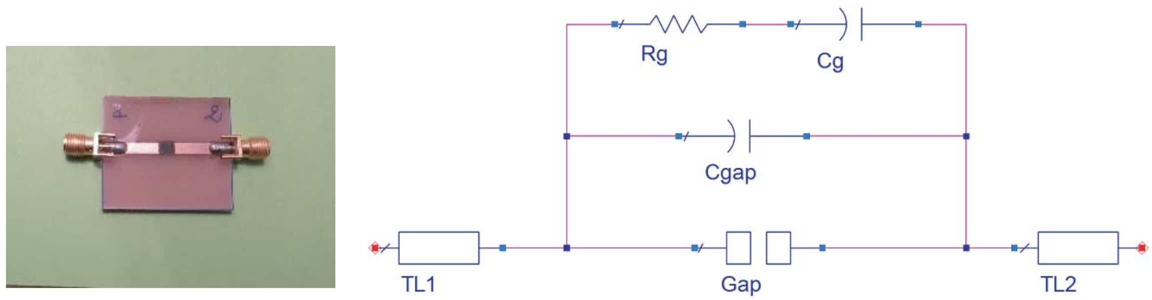

(a) (b)

Figure 1. (a) Microstrip line with gap loaded by a graphene thick film, and (b) equivalent circuit model.

The binder plays a crucial role in stabilizing the ink (by steric and thickening effects), ensuring the ink's printability and providing graphene platelets' interconnection and adherence on the substrate. Since film thermal treatment does not allow for binder removal (but only for solvent evaporation and cellulose chains reorganization above the glass transition temperature) the graphene platelets end up being embedded into the binder matrix. Therefore, the film's contribution to the overall microwave properties of the device is reasonably composed of two different effects: the dielectric losses stemming from the ethyl cellulose binder and the electrical conductivity of graphene platelets. For each of the graphene weight fractions (12.5% and 25%), three layers of film are deposited to realize a thickness of approximately 30 µm.

The measured transmission coefficient (S_{21}) for a line without any gap (reference line) and for microstrip lines with the gap filled with various film compositions is plotted in Fig. 2. These results emphasize that 12.5 wt.% graphene film acts as a binder insulator. On the other hand, 25 wt.% graphene film shows a marked increase in transmission across the gap due to the film's reduced sheet resistance. A circuit model for the graphene thick film is derived using Advanced Design System (ADS) simulations by fitting the amplitude and phase of the measured S-parameters. First, the line with a gap (no graphene film) is modeled using the microstrip gap, an additional capacitance ($C_{gap} = 0.01\,\text{pF}$) and microstrip line models available in ADS library. The 2.6 mm gap corresponds to $0.1\lambda_g$ at 5 GHz and can therefore be represented by an equivalent circuit. Capacitance, C_{gap}, accounts for the deviation of FR-4 substrate permittivity from its nominal value and its frequency dependence. This way, the fit between the measured S-parameter response and simulated equivalent circuit S-parameter response is improved. The binder across the gap and the 12.5 wt.% graphene film behave the same way as the microstrip line with an unloaded gap. For such low graphene concentrations, the dielectrics — the binder and the FR4 — have insignificant impacts on the S-parameter response. Since the loss tangent and relative dielectric constant of cellulose derivative binders are on the same order of the FR-4 [22], the electrical properties of the mirostrip line are not affected by introducing ethyl cellulose across the gap. Therefore, the difference between the microstrip line with the gap, the line with the binder only and the line with 12.5 wt.% graphene is negligible. On the other hand, 25 wt.% graphene film shows higher transmission due to the creation of percolative conductive paths across the two copper strips (in agreement with the DC sheet resistance). In addition, high graphene concentrations may result in the formation of nanoscale capacitors across the gap. Therefore, the film composed of 25 wt.% graphene can be represented with RC elements ($R_g = 290\,\Omega$, $C_g = 0.8\,\text{pF}$) in parallel as shown in Fig. 1(b). R_g represents the electrical resistance of the graphene conductive percolative structures, while C_g accounts for the combined effect of graphene and binder. In other words, graphene nanoplatelets act as the electrodes of a "classical" electrostatic nanocapacitor employing ethyl cellulose (and FR-4) as the dielectric. Therefore, capacitance C_g is not strictly attributed to the graphene. In fact, the chemical capacitance of graphene is inactive at microwave frequencies [23].

Measurements and model-derived fitted data are compared in Fig. 3 and Fig. 4 for the case of 12.5 wt.% and 25 wt.% graphene films, respectively. Good agreement is observed between the circuit model and the measurements over 1–5 GHz range.

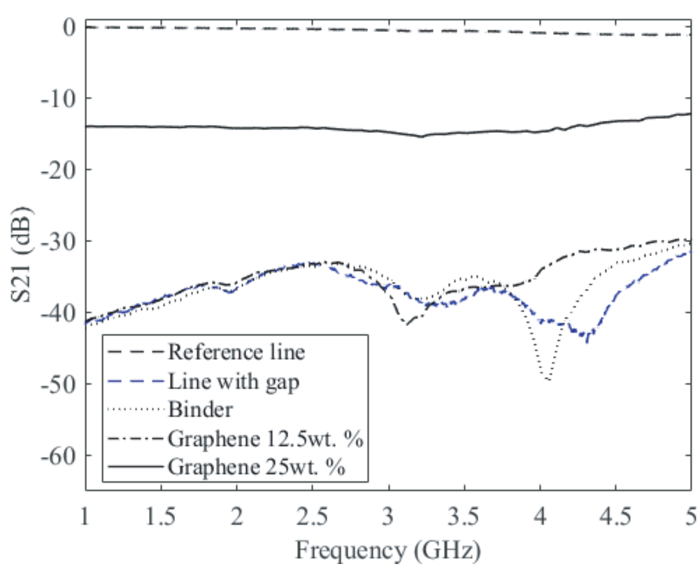

Figure 2. Measurement of the transmission coefficient magnitude of the reference line and of the microstrip line with gap for various graphene-loading compositions.

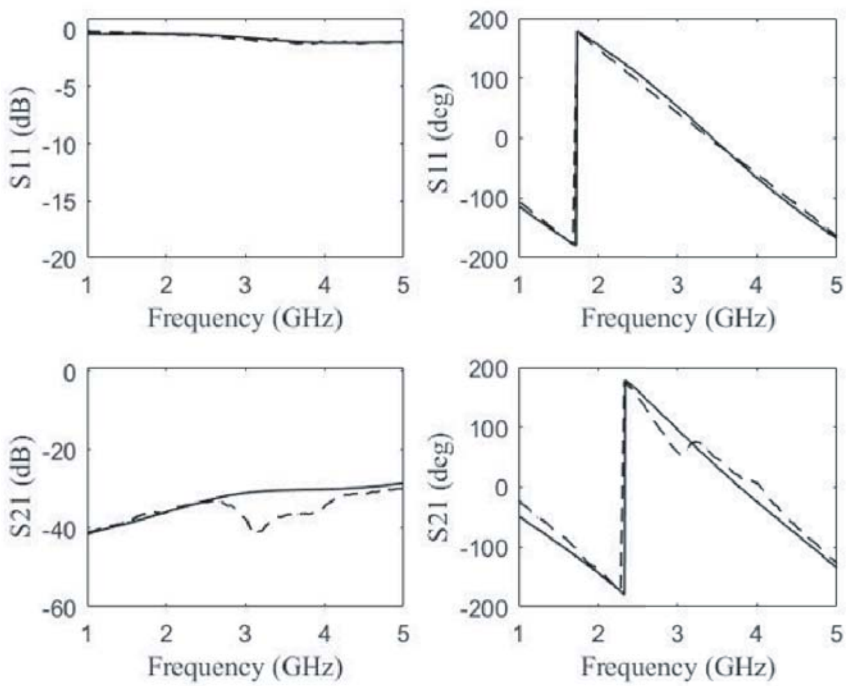

Figure 3. Measurements (dashed line) and simulations (solid line) for the film of graphene of weight fraction 12.5%.

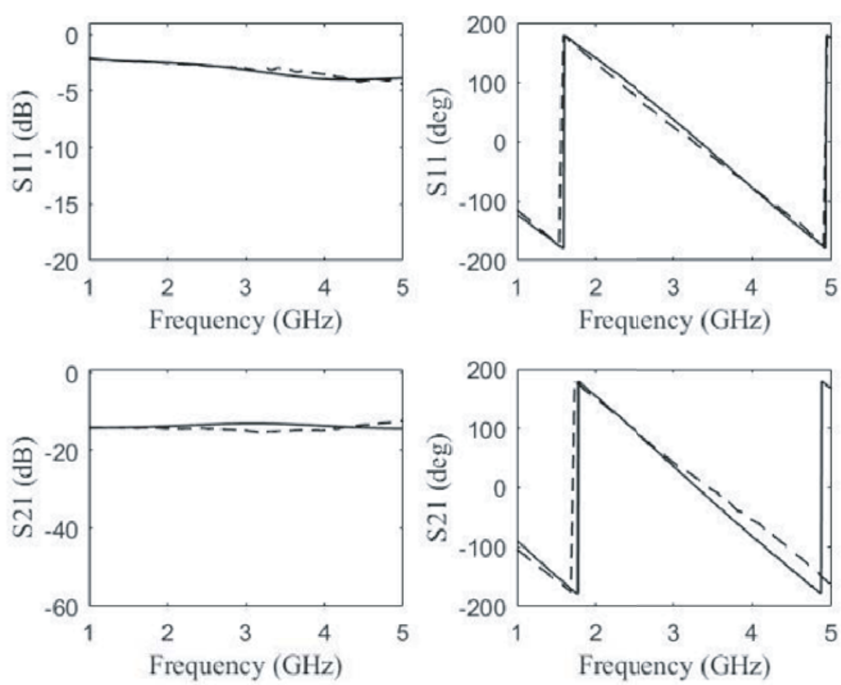

Figure 4. Measurements (dashed line) and simulations (solid line) for the film of graphene of weight fraction 25%.

4. CONCLUSION

A circuit model of thick films loaded with different amounts of graphene have been presented. Films made of binder alone, as well as binder plus graphene (weight fraction 12.5% and 25%), were printed across the gap of microstrip lines and experimentally studied to produce a circuit model in ADS. The S-parameter results reveal that low (12.5 wt.% upon the screen printing paste total mass) graphene loadings have negligible impact on the RF properties of the ethyl cellullose binder used for the polymer thick film deposition. Therefore, lightly loaded graphene films are prone to behave as lossy insulators where the dielectric loss is dominated by the substrate and binder. On the other hand, S-parameter measurements of 25 wt.% graphene films fit with an equivalent circuit composed of a single RC parallel element. Such a model can be easily ascribed to the formation of nano-capacitors composed of graphene nano-platelets distributed into an insulating matrix (film's binder and FR-4 substrate).

REFERENCES

1. Novoselov, K., A. Geim, S. Morozov, D. Jiang, Y. Zhang, S. Dubonos, I. Grigorieva, and A. Firsov, "Electric field effect in atomically thin carbon films," *Science*, Vol. 306, 666–669, 2004.
2. Geim, A., "Graphene: Status and prospects," *Science*, Vol. 324, 1530–1534, 2009.
3. Rafiee, M. A., J. Rafiee, Z. Wang, H. Song, Z.-Z. Yu, and N. Koratkar, "Enhanced mechanical properties of nanocomposites at low graphene content," *ACS Nano*, Vol. 3, 3884–3890, 2009.
4. Hyun, W. J., E. B. Secor, M. C. Hersam, C. D. Frisbie, L. F. Francis, "High-resolution patterning of graphene by screen printing with a silicon stencil for highly flexible printed electronics," *Advanced Materials*, Vol. 27, 109–1115, 2015.
5. Zinenko, T. L., A. Matsushima, and A. I. Nosich, "Surface-plasmon, grating-mode and slab-mode resonances in THz wave scattering by a graphene strip grating embedded into a dielectric slab," *IEEE J. Sel. Topics Quant. Electron.*, Vol. 23, No. 4, art. No. 4601809, 2017.
6. Bonaccorso, F., Z. Sun, T. Hasan, and A. C. Ferrari, "Graphene photonics and optoelectronics," *Nat. Photon.*, Vol. 4, 611–622, 2010.
7. Hill, E. W., A. Vijayaragahvan, and K. Novoselov, "Graphene sensors," *IEEE Sensors Journal*, Vol. 11, 3161–3170, 2011.
8. Zhu, Z., L. G.-Gancedo, A. J. Flewitt, H. Xie, F. Moussy, and W. I. Milne, "A critical review of glucose biosensors based on carbon nanomaterials: Carbon nanotubes and graphene," *Sensors*, Vol. 12, 5996–6022, 2012.
9. Leng, X., W. Li, D. Luo, and F. Wang, "Differential structure with graphene oxide for both humidity and temperature sensing," *IEEE Sensor Journal*, Vol. 17, 4357–4364, 2017.
10. Bozzi, M., L. Pierantoni, and S. Bellucci, "Applications of Graphene at microwave frequency," *Radioengineering*, Vol. 24, 661–669, 2015.
11. Hotopan, G., S. Ver Hoeye, C. Vazquez, R. Camblor, M. Fernandez, Las F. Heras, P. Alvarez, and R. Menendez, "Millimeter wave microstrip mixer based on graphene," *Progress In Electromagnetics Research*, Vol. 118, 57–69, 2011.
12. Hotopan, G., S. Ver Hoeye, C. Vazquez, A. Adaring, R. Camblor, M. Fernandez, F. R. Las Heras, "Millimeter wave subharmonic mixer implementation using graphene film coating," *Progress In Electromagnetics Research*, Vol. 140, 781–794, 2013.
13. Yasir, M., P. Savi, S. Bistarelli, A. Cataldo, M. Bozzi, L. Perregrini, and S. Bellucci, "A planar antenna with voltage-controlled frequency tuning based on few-layer graphene," *IEEE Antennas and Wireless Propagation Letters*, Vol. 16, 2380–2383, 2017.
14. Haider, N., N. D. Caratelli, and A. G. Yarovoy, "Recent developments in reconfigurable and multiband antenna technology," *Nanomaterials and Nanotechnology*, Vol. 869170, 1–9, 2016.
15. Hanson, G. W., "Dyadic Green's functions for an anisotropic, non-local model of biased graphene," *IEEE Transactions on antennas and propagation*, Vol. 56, No. 3, 747–757, March 2008.

16. Donelli, M. and G. Oliveri, "Design of tunable graphene-based antenna arrays for microwave applications," *IEEE International Symposium on Antennas and Propagation and USNC-URSI Radio Science meeeting*, 908–909, Memphis, Tennessee, USA, 2014.
17. Thomas, P., N. K. Pushkaran, and C. K. Aanandan, "Preparation and microwave characterization of novel polyaniline-graphene composite for antenna applications," *2017 Progress In Electromagnetics Research Symposium — Fall (PIERS — FALL)*, 1239–1244 Singapore, Nov. 19–22, 2017
18. Liang, M., M. Tuo, S. Li, Q. Zhu, and H. Xin, "Graphene conductivity characterization at microwave and THz frequency," *8th European Conference on Antennas and Propagation (EuCAP 2014)*, 489–491, The Hague, 2014.
19. Pierantoni, L., M. Dragoman, and D. Mencarelli, "Analysis of a microwave graphene-based patch antenna," *2013 European Microwave Conference*, 381–383, Nuremberg, 2013.
20. Savi, P., K. Naishadham, S. Quaranta, M. Giorcelli, and A. Bayat, "Microwave characterization of Graphene films for sensor applications," *IEEE International Instrumentation and Measurement Technology Conference (I2MTC)*, 1–5, Torino, Italy, May 22–25, 2017.
21. Savi, P., K. Naishadham, A. Bayat, M. Giorcelli, and S. Quaranta, "Multi-walled carbon nanotube thin film loading for tuning microstrip patch antennas," *European Conference on Antennas and Propagation (EuCAP)*, 1–3, Davos, Switzerland, Apr. 10–15, 2016.
22. Torgvonikov, I. G., "Dielectric properties of wood and wood-based materials," *Wood Science*, Vol. 35, No. 3, 135–143, Springer, 1993.
23. Pierantoni, L., D. Mencarelli, M. Bozzi, R. Moro, and S. Bellucci, "Graphene-based electronically tuneable microstrip attenuator," *Nanomaterials and Nanotechnology*, Vol. 4, No. 18, 1–6, 2014.